NATIONAL ADVISORY COMMITTEE FOR AERONAUTICS

TECHNICAL NOTE 2844

LAMINAR BOUNDARY LAYER ON CONE IN SUPERSONIC FLOW AT LARGE ANGLE OF ATTACK

By Franklin K. Moore

Lewis Flight Propulsion Laboratory
Cleveland, Ohio

Washington
November 1952

NATIONAL ADVISORY COMMITTEE FOR AERONAUTICS

TECHNICAL NOTE 2844

LAMINAR BOUNDARY LAYER ON CONE IN SUPERSONIC FLOW AT LARGE ANGLE OF ATTACK

By Franklin K. Moore

SUMMARY

The laminar boundary-layer flow about a circular cone at large angles of attack to a supersonic stream has been analyzed in the plane of symmetry by a method applicable in general to the flow about conical bodies.

At the bottom of the cone, velocity profiles were obtained showing the expected tendency of the boundary layer to become thinner on the under side of the cone as the angle of attack is increased.

At the top of the cone, the analysis failed to yield unique solutions, except for small angles of attack. Beyond a certain critical angle of attack, boundary-layer flow does not exist in the plane of symmetry, thus indicating separation. This critical angle is presented as a function of Mach number and cone vertex angle.

INTRODUCTION

The supersonic aerodynamics of pointed bodies has considerable current interest in connection with the design of aircraft and missile fuselages. An important feature of the flow about such bodies is the behavior of the boundary layer and, in particular, the flow separation which may occur along the low-pressure side of the body due to angle of attack. The present report will consider the development of the laminar boundary layer on the surface of a right circular cone at an angle of attack to a supersonic stream (see fig. 1). The conical configuration may be considered an idealization of the nose portion of a supersonic aircraft fuselage.

Outside a thin boundary layer on a cone, the nonviscous supersonic flow (upon which the boundary layer itself depends) is "conical" in the sense that physical quantities (such as velocity and pressure) are constant along any ray proceeding from the cone apex. The description of

this outer flow, contained in references 1 to 3 and elucidated in reference 4, is considered adequate for the purposes of this report, but subject to restrictions which will be discussed subsequently.

In figure 2 is shown qualitatively the circumferential pressure distribution on the cone surface predicted for various angles of attack (see reference 4). These pressure distributions depend only on the character of the nonviscous flow beyond the boundary layer, on the assumption that the boundary layer is extremely thin. When the angle of attack is very small, the pressure decreases monotonically from the bottom of the cone around to the top. For larger angles of attack there appears a region near the top of the cone wherein the pressure gradient reverses and the pressure increases toward the top. As the angle of attack is further increased, this region becomes greater in extent.

As a consequence of the conical nature of the nonviscous flow, it is shown in references 5 and 6 that the laminar boundary layer has parabolic similarity along generators of the cone; that is, velocity, pressure, and density inside the boundary layer are constant along any parabola (see fig. 1) drawn in any one meridional plane (plane passing through the body axis). Of course, circumferential variation of these quantities is to be expected when the cone is at angle of attack.

In reference 7 the effect of angle of attack on the laminar boundary layer is analyzed, in the limit of very small angle of attack, with the result that the boundary layer tends to be thicker on the top of the cone than on the bottom (fig. 3(a)). This is to be expected since the fluid near the base of the boundary layer has low inertia, is therefore inclined to follow the direction of the circumferential pressure gradient more closely than is the outer flow, and thus tends to drain away from beneath the cone and accumulate near the top. No separation is encountered because, for small angle of attack, the pressure gradient is always favorable (fig. 2(a)).

For larger angles of attack, when the pressure gradient reverses direction near the top of the cone (fig. 2(b)), experiment indicates the formation of boundary-layer "lobes" (fig. 3(b)). When the angle of attack is further increased, the lobe pattern finally breaks away from the body to form a vortex street (fig. 3(c)).

Recently (reference 8), at the Lewis laboratory a brief experiment was carried out in which a total-head probe was placed near the surface at the top of a cone and pointed toward the cone apex (fig. 4(a)). The cone was mounted in a supersonic wind tunnel, and the probe was used to measure the total head in the boundary layer at a fixed height above the surface as the angle of attack was varied by rotating the cone in the meridional plane containing the probe. Figure 4(b) shows the result of this test. The decrease in indicated total head as the angle

of attack was increased from negative to positive values may be interpreted to mean an increase in boundary-layer thickness at the top of the cone. Beyond a certain angle of attack, this tendency reverses, and the boundary layer apparently becomes thinner as the angle of attack is increased. This is a clear indication of the tendency to form lobes, as illustrated in figure 3(b).

In the present report of research conducted at the NACA Lewis laboratory, the laminar boundary layer in the meridional plane of symmetry of the flow is analyzed for large angles of attack in order to provide velocity profiles on the bottom of the cone and to provide a certain degree of insight into the question of separation on the top.

SOLUTION OF BOUNDARY-LAYER EQUATIONS IN PLANE OF SYMMETRY

Boundary-Layer Equations in Plane of Symmetry

In reference 7, it is shown that the dimensionless laminar boundary-layer equations for supersonic flow over a circular cone are

$$\left[f + \frac{1}{3\theta}\frac{p'(\varphi)}{p}g + \frac{2}{3\theta}g_{\varphi}\right]f_{\lambda\lambda} - \frac{2}{3\theta}g_{\lambda}f_{\lambda\varphi} + \frac{2}{3}(g_{\lambda})^2 + 2f_{\lambda\lambda\lambda} = 0 \tag{1a}$$

$$\left[f + \frac{1}{3\theta}\frac{p'(\varphi)}{p}g + \frac{2}{3\theta}g_{\varphi}\right]g_{\lambda\lambda} - \frac{2}{3\theta}g_{\lambda}g_{\lambda\varphi} - \frac{2}{3}g_{\lambda}f_{\lambda} - \frac{2}{3\theta}\frac{p'(\varphi)}{\rho} + 2g_{\lambda\lambda\lambda} = 0 \tag{1b}$$

$$T + (f_{\lambda})^2 + (g_{\lambda})^2 = T_1 + u_1^2 + w_1^2 \tag{1c}$$

$$p = \frac{\gamma-1}{2\gamma}\rho T \tag{1d}$$

Equations (1a) and (1b) are momentum equations, equation (1c) is an energy balance, and equation (1d) is the equation of state. A complete list of symbols is provided in appendix A. The functions $f(\lambda,\varphi)$ and $g(\lambda,\varphi)$ are related to the two-component vector potential discussed in reference 6 and are defined according to the relations

$$\left.\begin{aligned} u &= f_{\lambda} \\ w &= g_{\lambda} \end{aligned}\right\} \tag{2}$$

in a manner such as to satisfy the continuity equation identically.

The coordinate λ has been formed as follows:

$$\lambda \equiv \sqrt{3}\left[\left(\frac{p}{p_r}\right)^{-1/2}\int_0^y \rho\, dy\right]x^{-1/2} \tag{3}$$

The coordinate φ is the angle between the vertical plane of symmetry of the flow and any meridional plane of the body (fig. 1). Equations (1) and (3) imply that parabolic similarity of the Blasius type exits in meridional planes. As pointed out in references 5 and 6, this conclusion of parabolic similarity applies for the boundary layer on any smooth conically symmetric body in supersonic flow (for example, a cone of elliptic cross section).

In reference 7, all quantities are made dimensionless by referring them to the properties of the nonviscous flow at the outer edge of the boundary layer when the cone is at zero angle of attack. In the present report it will be convenient to use a different reference condition (subscript r) which will be defined subsequently. The following quantities on the left are to be identified with the dimensionless groups on the right:

$$\left.\begin{aligned} u,w &\sim u/u_r,\ w/u_r \\ \rho &\sim \rho/\rho_r \\ T &\sim 2c_pT/u_r^2 \\ p &\sim p/\rho_r u_r^2 \\ x,y &\sim \rho_r u_r x/C\mu_r,\ \rho_r u_r y/C\mu_r \end{aligned}\right\} \tag{4}$$

where the constant C arises from the assumption of the temperature-viscosity relation of Chapman and Rubesin (reference 9):

$$\frac{\mu}{\mu_r} = C\frac{T}{T_r} \tag{5a}$$

with C being defined as follows, in order to match equation (5a) to the Sutherland formula at the cone surface (denoted by subscript w):

$$C \equiv \left(\frac{T_w}{T_r}\right)^{\frac{1}{2}} \frac{1 + S/T_r}{T_w/T_r + S/T_r} \tag{5b}$$

The quantity S may be taken as equal to $(216^\circ\ R)2c_p/u_r^2$.

The following additional physical assumptions are embodied in equations (1):

(a) A thin boundary layer across which the static pressure is constant

(b) Prandtl number of 1 and constant ratio of specific heats γ

(c) No heat transfer through the surface

From equation (1c), since the case of Prandtl number of 1 and no heat transfer is considered, T_w in equation (5b) may be taken equal to the dimensionless stream stagnation temperature.

The boundary conditions on the functions $f(\lambda,\varphi)$ and $g(\lambda,\varphi)$ are: At the outer edge of the boundary layer, the u and w velocity components should take on the corresponding nonviscous values

$$f_\lambda(\infty,\varphi) = u_1(\varphi) \tag{6a}$$

$$g_\lambda(\infty,\varphi) = w_1(\varphi) \tag{6b}$$

At the cone surface, the u and w velocities should vanish

$$f_\lambda(0,\varphi) = g_\lambda(0,\varphi) = 0 \tag{6c}$$

and the normal velocity v should vanish. It is shown in reference 6 that this last requirement is met if

$$f(0,\varphi) = g(0,\varphi) = 0 \tag{6d}$$

Equations (1), involving two independent variables, would be quite difficult to solve in general. However, a certain amount of information can be obtained by restricting consideration to the plane of symmetry, thus yielding a tractable set of ordinary equations involving λ as the only independent variable.

In the plane of symmetry $\varphi = 0,\pi$, $w = g_\lambda = 0$. Because $u = f_\lambda$ is even about the plane of symmetry and may be expected to be regular there, $f_{\lambda\varphi} = 0$. The pressure and the density are also even, and therefore $p'(\varphi)$ vanishes at $\varphi = 0,\pi$. Thus, in the plane of symmetry, equation (1a) reduces to the following equation:

$$\left(f + \frac{2}{3\theta} g_\varphi\right) f_{\lambda\lambda} + 2f_{\lambda\lambda\lambda} = 0 \tag{7a}$$

Every term in equation (1b) vanishes at the plane of symmetry; and, therefore, in order to obtain a meaningful equation, it is necessary first to differentiate equation (1b) with respect to φ and then drop terms which vanish at $\varphi = 0,\pi$. This procedure yields the following result:

$$\left(f + \frac{2}{3\theta} g_{\varphi}\right) g_{\lambda\lambda\varphi} - \frac{2}{3\theta}\left(g_{\lambda\varphi}\right)^2 - \frac{2}{3} g_{\lambda\varphi} f_{\lambda} - \frac{2}{3\theta} \frac{p''(\varphi)}{\rho} + 2g_{\lambda\lambda\lambda\varphi} = 0 \tag{7b}$$

Equation (1c) becomes

$$T + (f_{\lambda})^2 = T_1 + u_1^2 \tag{7c}$$

Equations (7) may be considered a set of ordinary differential equations for the functions $f(\lambda,0)$ and $g_{\varphi}(\lambda,0)$, or $f(\lambda,\pi)$ and $g_{\varphi}(\lambda,\pi)$, depending on whether the solution is required at the bottom or the top of the cone. According to equations (2), the result $f(\lambda,0 \text{ or } \pi)$ may be differentiated with respect to λ to give the profile of meridional velocity u in the plane of symmetry. The form assumed by the circumferential velocity profile w as $\varphi \to 0$ or π is given by $g_{\varphi\lambda}(\lambda,0 \text{ or } \pi)$ in the sense that, at a small angular distance $d\varphi$ away from the plane of symmetry, $w \approx g_{\varphi\lambda}\, d\varphi$.

The boundary conditions (equations (6)) become, in the plane of symmetry,

$$\left.\begin{aligned} &f_{\lambda}(\infty,0 \text{ or } \pi) = u_1(0 \text{ or } \pi) \\ &g_{\varphi\lambda}(\infty,0 \text{ or } \pi) = w_{1_{\varphi}}(0 \text{ or } \pi) \\ &f_{\lambda}(0,0 \text{ or } \pi) = g_{\varphi\lambda}(0,0 \text{ or } \pi) = f(0,0 \text{ or } \pi) = g_{\varphi}(0,0 \text{ or } \pi) = 0 \end{aligned}\right\} \tag{8}$$

In view of the first of equations (8) and of equation (7c), it is convenient to specify the reference condition (subscript r) to be that existing at the outer edge of the boundary layer, for the particular angle of attack under consideration, evaluated at either $\varphi = 0$ or $\varphi = \pi$, depending on whether the analysis pertains to the bottom or top of the cone.

Because the pressure is assumed constant across the boundary layer, equations (1d) and (7c) and the assumption of constant pressure across the boundary layer $(p = p_1)$ provide that

$$\frac{1}{\rho} = \frac{T}{T_1} = 1 + \frac{1}{T_1}\left[1 - (f_{\lambda})^2\right] \tag{9}$$

From conventions (4), $T_1 = \left(\frac{2}{\gamma-1}\right)\Big/ M_1^2$. For convenience, the following definitions are made:

$$g_\varphi(\lambda, 0 \text{ or } \pi) \equiv \frac{3\theta}{2} k\psi(\lambda) \tag{10a}$$

$$k \equiv \frac{2}{3\theta} w_{1_\varphi}(0 \text{ or } \pi) \tag{10b}$$

Equation (9) and definitions (10) are introduced into equations (7a) and (7b), and a value of $p''(0 \text{ or } \pi)$ is assigned consistent with the nonviscous equations at the outer edge of the boundary layer ($p''(0 \text{ or } \pi)$ may conveniently be obtained from equations (1b) and (6) by setting $g_{\varphi\lambda\lambda} = g_{\varphi\lambda\lambda\lambda} = 0$ when $\lambda = \infty$).

The following pair of simultaneous ordinary differential equations then result:

$$(f + k\psi)f'' + 2f''' = 0 \tag{11a}$$

$$(f + k\psi)\psi'' + 2\psi''' - k(\psi')^2 - \frac{2}{3}\psi'f' + \left(k + \frac{2}{3}\right)\left\{1 + \frac{1}{T_1}\left[1 - (f')^2\right]\right\} = 0 \tag{11b}$$

and boundary conditions (8) become

$$f'(\infty) = \psi'(\infty) = 1 \tag{12a}$$

$$f'(0) = \psi'(0) = 0 \tag{12b}$$

$$f(0) = \psi(0) = 0 \tag{12c}$$

Two parameters appear: k, which depends essentially on angle of attack, and T_1, which is essentially dependent on Mach number. If the angle of attack (and hence k) is zero or nearly zero, equations (11) become precisely those considered in reference 7 and may be solved quite readily, since equation (11b) becomes linear and the solution of equation (11a) is well known as the Blasius function. When k differs substantially from zero (moderate or large angle of attack), equations (11) are both nonlinear and the solutions are interdependent. For any particular case, when only the stream Mach number, cone vertex angle, and angle of attack are specified, the parameters k and T_1 must be obtained by recourse to a theory of the outer nonviscous flow.

Outer Nonviscous Flow

In references 1 to 3, the results of a theory of nonviscous supersonic flow about circular cones at angle of attack are tabulated. The

case of zero angle of attack (reference 1) is solved exactly in the sense that no assumption of small vertex angle is made. The equations are then expanded in powers of angle of attack with the use of the zero-angle-of-attack solution as the first approximation. Terms linear in angle of attack are presented in reference 2, and terms proportional to the square of angle of attack are presented in reference 3. Reference 4 clarifies the application of the theory to the computation of flow conditions at the cone surface.

There are two objections to the use of this theory in the present application:

(1) Neglect of terms in the expansion beyond that involving the square of angle of attack may lead to an insufficiently accurate representation of the flow at the large angles of attack which are of interest. Unfortunately, no nonviscous theory is available that treats the effect of angle of attack with greater precision. In reference 4, a comparison of the theoretical and experimental pressure distributions is presented for a cone of semivertex angle of 10°, at a Mach number of 2, and of an angle of attack of 12.2°. The agreement shown is very good, especially since the angle of attack is sufficiently large that the pressure distribution is of the type shown in figure 2(b).

(2) In reference 10, Ferri points out that the method of expansion used in references 2 and 3 is improper near the cone surface and leads to an erroneous form of the entropy distribution around the cone. Therefore, the theory cannot be applied if the vertex angle, the angle of attack, or the Mach number is so large that the flow may not be considered essentially isentropic. In reference 7, an argument is presented to the effect that in the limit of infinitesimal angle of attack the presence of a boundary layer ensures that the error in entropy distribution is of no consequence even for large cone vertex angles. That argument in no way applies to the present analysis because the angles of attack considered are not infinitesimal. For the purposes of this report, the use of references 2 and 3 in their present form is justified only in cases for which isentropic flow may be assumed.

According to reference 4, the velocity components at the cone surface are, using the notation of references 1 to 3 for quantities tabulated therein,

$$\frac{u_1(\varphi)}{\bar{u}} = 1 + \alpha \frac{x}{\bar{u}} \cos \varphi + \alpha^2 \left[\frac{u_0}{\bar{u}} + \frac{1}{2} \frac{x}{\bar{u}} \cot \Theta + \frac{1}{2} + \left(\frac{u_2}{\bar{u}} - \frac{1}{2} \frac{x}{\bar{u}} \cot \Theta + \frac{1}{2} \right) \cos 2\varphi \right] + \cdots \tag{13}$$

$$\frac{w_1(\varphi)}{\bar{u}} = \alpha \frac{z}{\bar{u}} \sin \varphi + \alpha^2 \left[\frac{w_2}{\bar{u}} - \csc \Theta - \frac{z}{\bar{u}} \cot \Theta \right] \sin 2\varphi + \cdots \quad (14)$$

The pressure and density are

$$\frac{p_1(\varphi)}{\bar{p}} = 1 + \alpha \frac{\eta}{\bar{p}} \cos \varphi + \alpha^2 \left[\frac{p_0}{\bar{p}} + \frac{\gamma}{2} \bar{M}^2 + \frac{1}{2} \frac{\eta}{\bar{p}} \cot \Theta + \left(\frac{p_2}{\bar{p}} + \frac{\gamma}{2} \bar{M}^2 - \frac{1}{2} \frac{\eta}{\bar{p}} \cot \Theta \right) \cos 2\varphi \right] + \cdots \quad (15)$$

$$\frac{\rho_1(\varphi)}{\bar{\rho}} = 1 + \alpha \frac{\xi}{\bar{\rho}} \cos \varphi + \alpha^2 \left[\frac{\rho_0}{\bar{\rho}} + \frac{1}{2} \bar{M}^2 + \frac{1}{2} \frac{\xi}{\bar{\rho}} \cot \Theta + \left(\frac{\rho_2}{\bar{\rho}} + \frac{1}{2} \bar{M}^2 - \frac{1}{2} \frac{\xi}{\bar{\rho}} \cot \Theta \right) \cos 2\varphi \right] + \cdots \quad (16)$$

The barred quantities are those pertaining to the case of zero angle of attack. From equations (10b), (13), and (14),

$$k = \frac{2}{3\theta} \frac{\pm \alpha \frac{z}{\bar{u}} + 2\alpha^2 \left(\frac{w_2}{\bar{u}} - \frac{1}{\theta} - \frac{\sqrt{1 - \theta^2}}{\theta} \frac{z}{\bar{u}} \right)}{1 \pm \alpha \frac{x}{\bar{u}} + \alpha^2 \left(1 + \frac{u_0}{\bar{u}} + \frac{u_2}{\bar{u}} \right)} + \cdots$$

or, approximately,

$$k = \frac{2}{3} \left[\pm \frac{\alpha}{\theta} \frac{z}{\bar{u}} + 2\alpha^2 \left(\frac{w_2}{\theta \bar{u}} - \frac{1}{\theta^2} - \frac{\sqrt{1 - \theta^2}}{\theta^2} \frac{z}{\bar{u}} - \frac{1}{2\theta} \frac{xz}{\bar{u}^2} \right) \right] + \cdots \quad (17)$$

The plus or minus sign refers to $\varphi = 0$ or π, respectively. From conventions (4), equations (13), (15), and (16), and the result of reference 1 that $1/\bar{T} = \bar{u}^2/(1 - \bar{u}^2) = \frac{\gamma - 1}{2} \bar{M}^2$,

$$\frac{1}{T_1} = \frac{1}{\bar{T}} \frac{M_1^2}{\bar{M}^2} = \frac{u^2}{1 - \bar{u}^2} \left(\frac{u_1}{\bar{u}} \right)^2 \frac{\bar{p}}{p_1} \frac{\rho_1}{\bar{\rho}}$$

$$= \frac{\bar{u}^2}{1 - \bar{u}^2} \frac{\left[1 \pm \alpha \frac{x}{\bar{u}} + \alpha^2 \left(1 + \frac{u_0}{\bar{u}} + \frac{u_2}{\bar{u}} \right) \right]^2 \left[1 \pm \alpha \frac{\xi}{\bar{\rho}} + \alpha^2 \left(\frac{\rho_0}{\bar{\rho}} + \frac{\rho_2}{\bar{\rho}} + \frac{2}{\gamma - 1} \frac{\bar{u}^2}{1 - \bar{u}^2} \right) \right]}{1 \pm \alpha \frac{\eta}{\bar{p}} + \alpha^2 \left(\frac{p_0}{\bar{p}} + \frac{p_2}{\bar{p}} + \frac{2\gamma}{\gamma - 1} \frac{\bar{u}^2}{1 - \bar{u}^2} \right)} + \cdots$$

or, approximately,

$$\frac{1}{T_1} = \frac{\bar{u}^2}{1 - \bar{u}^2}\left\{1 \pm \alpha\left(2\frac{x}{\bar{u}} + \frac{\xi}{\bar{\rho}} - \frac{\eta}{\bar{p}}\right) + \alpha^2\left[2\left(1 + \frac{u_0}{\bar{u}} + \frac{u_2}{\bar{u}}\right) + \frac{\rho_0}{\bar{\rho}} + \frac{\rho_2}{\bar{\rho}} - \frac{p_0}{\bar{p}} - \frac{p_2}{\bar{p}} - 2\frac{\bar{u}^2}{1 - \bar{u}^2} + 2\frac{x}{\bar{u}}\left(\frac{\xi}{\bar{\rho}} - \frac{\eta}{\bar{p}}\right) + \frac{x^2}{\bar{u}^2} + \frac{\eta^2}{\bar{p}^2} - \frac{\eta}{\bar{p}}\frac{\xi}{\bar{\rho}}\right]\right\} + \cdots \tag{18}$$

In figure 5 are shown k and $1/T_1$ as functions of α for a cone of semivertex angle of 7.5° and a stream Mach number of 3.1. From the tabulations of reference 2, it may be inferred that under these conditions the isentropic assumption leads to errors of less than 1 percent in quantities proportional to the angle of attack.

Solution of Equations at $\varphi = 0$

Equations (11) have been solved, subject to boundary conditions (12), at $\varphi = 0$ and various angles of attack for a cone of semivertex angle of 7.5° and a stream Mach number of 3.1 for which the values of k and $1/T_1$ are given in figure 5. The computations were carried out by Dr. Lynn Albers of the Lewis laboratory and are described in appendix B. The resulting boundary-layer profiles of meridional velocity u and gradient of circumferential velocity $\partial w/\partial\varphi$ are shown in figure 6. The curves for $\alpha = 0$ are obtained from reference 7. The profiles show clearly that, as the angle of attack is increased, the boundary layer becomes thinner on the bottom of the cone, and the shear stress at the wall increases.

Skin friction. - The meridional and circumferential components of the viscous shear stress at the bottom of the cone surface may be written in coefficient form as follows:

$$\left[C_{f_x}\right]_{\varphi=0} = \frac{1}{\frac{1}{2}\rho_1 u_1^2}\left(\mu\frac{\partial u}{\partial y}\right)_{\substack{y=0\\ \varphi=0}}$$

$$\left[C_{f_\varphi}\right]_{\varphi=0} = 0$$

$$\left[\frac{\partial C_{f_\varphi}}{\partial\varphi}\right]_{\varphi=0} = \frac{1}{\frac{1}{2}\rho_1 u_1^2}\left[\mu\frac{\partial}{\partial y}\left(\frac{\partial w}{\partial\varphi}\right)\right]_{\substack{y=0\\ \varphi=0}}$$

where the quantities on the right are in dimensional form. Application of equations (1d), (2), (3), (4), (5), and (10a) yields

$$\sqrt{\frac{R_x}{3C}}\left[C_{f_x}\right]_{\varphi=0} = 2f''(0) \tag{19a}$$

$$\left[C_{f_\varphi}\right]_{\varphi=0} = 0 \tag{19b}$$

$$\sqrt{\frac{R_x}{3C}}\left[\frac{\partial C_{f_\varphi}}{\partial \varphi}\right]_{\varphi=0} = 3\theta k\psi''(0) \tag{19c}$$

where

$$R_x \equiv \frac{\rho_1 u_1 x}{\mu_1}$$

Variation of these skin-friction coefficients with angle of attack is shown in figure 7 for a particular case.

Displacement thickness. - In reference 11 it is shown that the displacement thickness Δ for a cone at angle of attack is the solution of the equation

$$\frac{3}{2}\theta\rho_1 u_1(\Delta - \delta_x) + \frac{\partial}{\partial\varphi}\left[\rho_1 w_1(\Delta - \delta_\varphi)\right] = 0 \tag{20}$$

where

$$\left.\begin{aligned}\delta_x &\equiv \int_0^\infty \left(1 - \frac{\rho u}{\rho_1 u_1}\right)dy \\ \delta_\varphi &\equiv \int_0^\infty \left(1 - \frac{\rho w}{\rho_1 w_1}\right)dy\end{aligned}\right\} \tag{21}$$

At $\varphi = 0$, $w_1 = 0$ and equation (20) may be solved directly

$$\Delta = \frac{\delta_x + k\delta_\varphi}{1 + k} \tag{22}$$

where k is defined in equation (10b). From equations (5) and (9), with δ_x defined in terms of a Reynolds number,

$$R_{\delta_x} \equiv \frac{\rho_1 u_1 \delta_x}{\rho_1}$$

$$R_{\delta_x} = \sqrt{\frac{CR_x}{3}} \int_0^{\infty} \left[1 - f' + \frac{1}{T_1}(1 - f'^2)\right] d\lambda \qquad (23a)$$

Using equations (10) and applying l'Hospital's rule to evaluate at $\varphi = 0$ the limit of the ratio w/w_1 appearing in equation (21) yield

$$R_{\delta_\varphi} = \sqrt{\frac{CR_x}{3}} \int_0^{\infty} \left[1 - \psi' + \frac{1}{T_1}(1 - f'^2)\right] d\lambda \qquad (23b)$$

Therefore,

$$\sqrt{\frac{3}{CR_x}} R_\Delta = \int_0^{\infty} \left\{ \frac{k}{1+k}(f' - \psi') + (1 - f') \left[1 + \frac{1}{T_1}(1 + f')\right] \right\} d\lambda \qquad (23c)$$

Figure 8 shows the variation of displacement thickness with angle of attack for a particular case and again illustrates the expected progressive shift of the boundary layer from bottom to top as the angle of attack is decreased.

Failure of Method at $\varphi = \pi$

Except for quite small angles of attack, equations (11) cannot be solved at the top of the cone ($\varphi = \pi$). Over part of the range of angle of attack, the solutions are indeterminate; and, beyond a certain angle of attack, the solutions do not exist at all. These properties of equations (11) will be demonstrated and discussed in the following paragraphs.

Asymptotic forms of equations. - The difficulties just mentioned may best be inferred from the asymptotic forms of equations (11) at large λ. From equation (12a) it is clear that, for large λ, f and ψ may be written as follows:

$$f = \lambda + F(\lambda)$$

$$\psi = \lambda + \Psi(\lambda)$$

where $F'(\infty) = \psi'(\infty) = 0$. Substitution into equations (11) yields the asymptotic forms for large λ

$$(1 + k)\lambda F'' + 2F''' = 0 \tag{24a}$$

$$(1 + k)\lambda \Psi'' + 2\Psi''' - 2\left(k + \frac{1}{3}\right)\Psi' = \frac{2}{3} F'\left[1 + \frac{3}{T_1}\left(k + \frac{2}{3}\right)\right] \tag{24b}$$

Indeterminate solutions. - Consideration will now be given to the problem of obtaining the complementary solution of equation (24b). Defining a new dependent variable

$$G \equiv e^{\frac{1+k}{8}\lambda^2} \Psi'$$

yields the equation

$$G'' - \left[\frac{5}{4} k + \frac{7}{12} + \left(\frac{1 + k}{4}\right)^2 \lambda^2\right] G = 0 \tag{25}$$

This is essentially Weber's equation (reference 12, paragraph 16.5), and the asymptotic solutions are

$$e^{-\frac{1+k}{8}\lambda^2}\left(\sqrt{\frac{1+k}{2}}\lambda\right)^{-3\frac{k+5/9}{1+k}}$$

$$e^{\frac{1+k}{8}\lambda^2}\left(\sqrt{\frac{1+k}{2}}\lambda\right)^{2\frac{k+1/3}{1+k}}$$

Thus, the asymptotic complementary solutions of equation (24b) are

$$\Psi' = e^{-\frac{1+k}{4}\lambda^2}\left(\sqrt{\frac{1+k}{2}}\lambda\right)^{-3\frac{k+5/9}{1+k}} \tag{26a}$$

$$\Psi' = \left(\sqrt{\frac{1+k}{2}}\lambda\right)^{2\frac{k+1/3}{1+k}} \tag{26b}$$

Because it is required that $\Psi'(\infty) = 0$, solution (26b) is rejected when $k > -1/3$. If $k < -1/3$, both solutions may be retained, and an additional undetermined constant appears. When $k > 0$ (at the bottom of the cone), the complete solution of equations (11) exists and is unique, and solution (26b) is to be rejected in forming the asymptotic solution. Therefore, if solution (26b) and the associated constant must be retained

when $k < -1/3$, it is clear that the complete solution for $k < -1/3$ cannot be unique. This indeterminacy has been verified by numerical integration of equations (11), as described in appendix B.

This indeterminacy arises because essential information has been lost by specializing the equations to apply only in the plane of symmetry. When the equations are so written, it is implied that the boundary-layer development in the plane of symmetry is affected only by conditions in that plane. The lateral region of influence of points on the body in the plane of symmetry grows parabolically (the shaded regions in sketches (a) and (b)), according to the law of molecular diffusion,

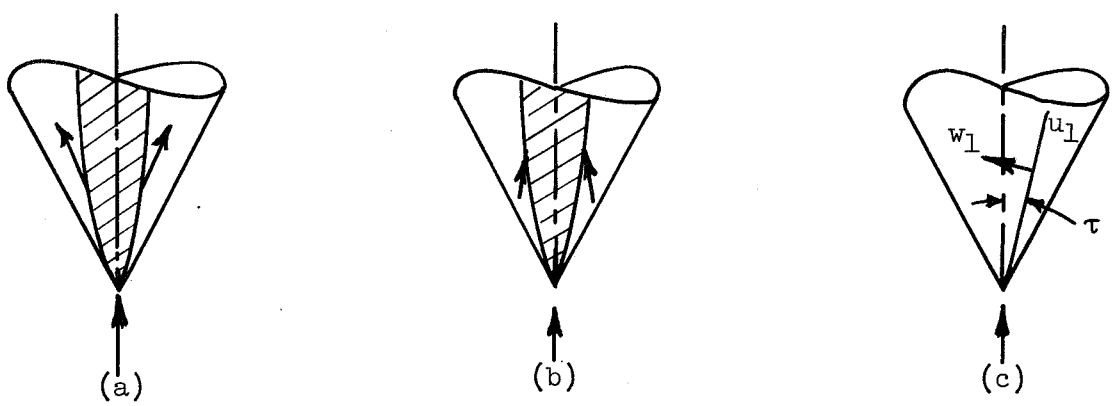

Top view of cone ($\varphi = \pi$) at positive angle of attack.

when, as in the present instance, there is no pressure gradient in the stream direction. Fluid enters the boundary layer from the outer stream. If the fluid then moves laterally (because of the angle of attack) out of the region of influence of the plane of symmetry, as shown in sketch (a), the flow is uniquely determined by outer stream conditions in the plane of symmetry. Clearly, this is the case when $\varphi = \pi$ and α is small, and when $\varphi = 0$ and α has any positive value. When $\varphi = \pi$, except for small angles of attack, the lateral motion of the fluid is inward relative to the region of influence, as shown in sketch (b). This fluid then brings into the region of influence of the plane of symmetry information concerning boundary-layer development as it proceeds around the cone from the bottom. Consequently, outer stream conditions at $\varphi = \pi$ may not uniquely determine the boundary-layer characteristics at $\varphi = \pi$, and indeterminate solutions of equations (11) may be anticipated.

The condition $k = -1/3$ specifies an angle of attack such that, at $\varphi = \pi$, the outer flow streamlines are just tangent to the parabolic region of influence. This statement may be proved as follows: From definition (10b), if $k = -1/3$, then $w_{1\varphi}/u_1 = -\theta/2$. Near $\varphi = \pi$ (see sketch (c)),

$w_1 = w_{1_\varphi} d\varphi = - w_{1_\varphi} \frac{\tau}{\theta}$. Thus, when $k = -1/3$, $w_1/u_1 = \tau/2$. From this last equation and the geometrical properties of parabolas, it may be inferred that the streamlines are parabolas with focus at the cone apex. Therefore, the situation shown in sketch (b) applies if $k < - 1/3$ and equations (11) have no unique solution.

If $k \geq - 1/3$, it might be inferred that equations (11) may be solved uniquely. However, the condition $k \geq - 1/3$ is not sufficient, but, rather, only necessary for uniqueness. Inspection of the profiles shown in figure 6 for $\alpha = k = 0$ indicates that, for $0 > k \geq - 1/3$, the streamlines within the boundary layer may be expected to incline more sharply toward the plane $\varphi = \pi$ than do the streamlines near the edge of the boundary layer, and thus may bring information from beneath the cone even though the outer ones do not. Therefore, the necessary condition for uniqueness would be (see equations (2) and (10a)):

$$\left(\frac{w_\varphi}{u}\right)_{max} = \frac{3}{2} \theta k \left(\frac{\psi'(\lambda)}{f'(\lambda)}\right)_{max} > - \frac{\theta}{2}$$

or,

$$k > - \frac{1}{3} \Bigg/ \left(\frac{\psi'}{f'}\right)_{max} \tag{27a}$$

Figure 6 indicates that perhaps the maximum value of ψ'/f' is to be found at $\lambda = 0$, in which case criterion (27a) would become

$$k > = \frac{1}{3} \frac{f''(0)}{\psi''(0)} \tag{27b}$$

Nonexistent solutions. - The solution of equation (24a) is

$$F'' = e^{- \frac{1+k}{4} \lambda^2}$$

The requirement that $F''(\infty) = 0$ is met only if $k > - 1$. If $k \leq - 1$, no solution of equation (24a) exists which satisfies the boundary conditions, and, therefore, the Prandtl boundary-layer equations fail to describe the flow. This was first pointed out by Hayes in reference 5. The Prandtl equations differ from the exact equations essentially in that a thin boundary layer is assumed. Thus, if $k \leq - 1$, the boundary layer cannot be regarded as thin. It may be noted that equation (22) implies that, as $k \to - 1$, the displacement thickness approaches infinity.

Any boundary layer grows by the entrainment of fluid at its outer edge. That is, fluid particles acquire vorticity by entry into the boundary layer. The reverse process cannot occur - fluid particles cannot leave the boundary layer, thus losing their vorticity. In the case under consideration, it will be shown that when $k < -1$, the streamlines at the outer edge of the boundary layer would proceed outward relative to the boundary layer, if the boundary layer were to retain parabolic similarity. Because such a situation is physically impossible, the Prandtl equations fail to yield a solution.

From reference 11, the normal velocity at the outer edge of the boundary layer at $\varphi = \pi$ is

$$v_1 \cong u_1 \frac{\partial \Delta}{\partial x} + (h - \Delta)\left(\frac{\partial v_1}{\partial y}\right)_{y=0} \tag{28}$$

where h is a somewhat arbitrary definition of the outer edge of the boundary layer and $\left(\frac{\partial v_1}{\partial y}\right)_{y=0}$ is obtained from analysis of the outer nonviscous flow. The equation of continuity for the outer flow, evaluated at the surface of the cone in the plane of symmetry, may be written

$$\frac{u_1}{x} + \frac{1}{\theta x}\frac{\partial w_1}{\partial \varphi} + \left(\frac{\partial v_1}{\partial y}\right)_{y=0} = 0 \tag{29}$$

With equations (28) and (29) combined, the flow inclination at the outer edge of the boundary layer is

$$\frac{v_1}{u_1} = \frac{\partial \Delta}{\partial x} - \frac{h - \Delta}{x}\left(1 + \frac{1}{\theta u_1}\frac{\partial w_1}{\partial \varphi}\right) \tag{30}$$

The Prandtl (thin) boundary layer may be expected to exist only if

$$\frac{\partial h}{\partial x} > \frac{v_1}{u_1}$$

or, with equation (30) introduced, if

$$\frac{1}{\theta u_1}\frac{\partial w_1}{\partial \varphi} > -\left[1 + \frac{x}{h - \Delta}\frac{\partial}{\partial x}(h - \Delta)\right] \tag{31}$$

If parabolic similarity is assumed (h and Δ each proportional to $\sqrt{x}$), inequality (31) becomes

$$\frac{1}{\theta u_1}\frac{\partial w_1}{\partial \varphi} > -\frac{3}{2}$$

or, from equation (10b),

$$k > -1$$

SEPARATION

The critical condition $k = -1$ might be expected to be of physical as well as analytical significance because some sort of catastrophic thickening of the boundary layer is implied. In particular, this critical condition may reasonably be supposed to be connected with the phenomenon of laminar separation. In order to explore this possibility, it is first necessary to describe qualitatively what is meant by separation in three-dimensional boundary-layer flow. Difficulty has been encountered in establishing a satsifactory qualitative criterion for three-dimensional separation (see, for example, reference 5). Therefore, in the subsequent paragraphs, the general problem of three-dimensional separation will be discussed, and then the particular case of the cone at angle of attack will be considered.

General Considerations

Plane flow. - In plane flow, separation is customarily identified by the appearance of reverse flow (sketch (d)). In order to generalize this concept to three-dimensional flow, it is necessary to consider the separated region as a whole. In plane flow, the separation point of sketch (d) might be regarded as the forward boundary of a vortex sheet embedded, or encapsulated, within a region bounded by the body and a stream surface meeting the body (sketch (e). Sketch (e) shows separation followed by reattachment. Of course, the sort of separation of greatest engineering importance occurs when such an embedded vortex sheet rolls up to form a large concentrated vortex, or is shed as a vortex street, with the consequence that the outer flow is greatly disturbed and a large pressure effect (form drag) occurs.

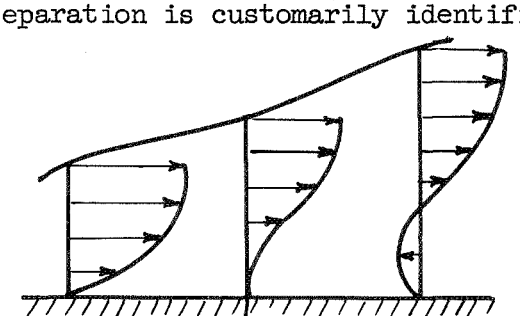

(d) Velocity profiles in plane flow.

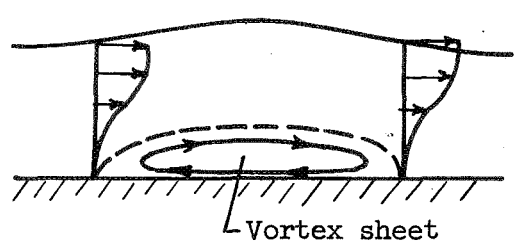

(e) Embedded separation region.

If a boundary-layer solution of the type shown in sketch (e) were obtained, there would be little theoretical expectation of "rolling up". That is, a vortex sheet completely embedded in a thin boundary layer would be constrained to remain flat against the body. However, if the theoretically predicted vortex sheet extends downstream into a region where the thin boundary-layer equations do not apply (that is, where the solution "blows up" predicting an infinitely thick boundary layer), then in that region the vortex sheet would not be constrained to lie flat and the rolling-up process could occur.

The foregoing discussion seems to provide the proper description of what occurs behind a bluff body: A complete solution of the thin laminar boundary-layer equations for the flow over a cylinder would probably yield a streamline pattern of the form shown in sketch (f). The boundary layer would be predicted to gain mass flow by entrainment as it proceeds around the body, until it reaches the vicinity of the rear stagnation point. There, the mass flow contained in the boundary layer must finally leave the body and proceed downstream. The boundary layer therefore cannot remain theoretically thin, but rather must approach infinite thickness in violation of the Prandtl assumptions. In this region, then, the aft boundaries of the pair of vortex sheets are free to roll up into concentrated vortices, thus distorting the outer flow in such a way that the rolling-up process engulfs most of the region which would otherwise be occupied by a flat vortex sheet. The leading edge of the sheet, however, is still constrained to lie flat against the body.

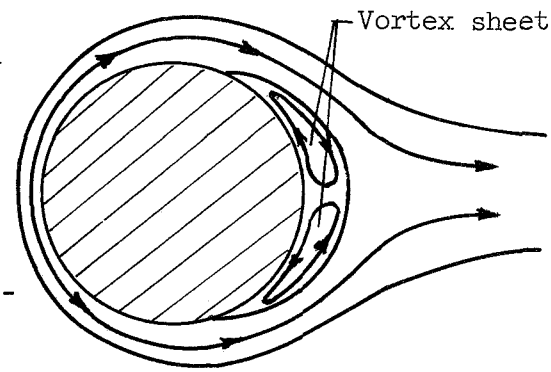

(f) Possible boundary-layer solution for cylinder.

Three-dimensional flow. - The foregoing description of plane separation may be generalized to three-dimensional flow as follows: A separated region on a three-dimensional body consists of a vortex sheet embedded between the body surface and a stream surface attached to the body in a closed curve, as shown in sketch (g), which is a view of the body from above. The arrows indicate the direction of resultant shear stress at the surface and outside the separated region. The situation shown in the sketch would correspond to separation

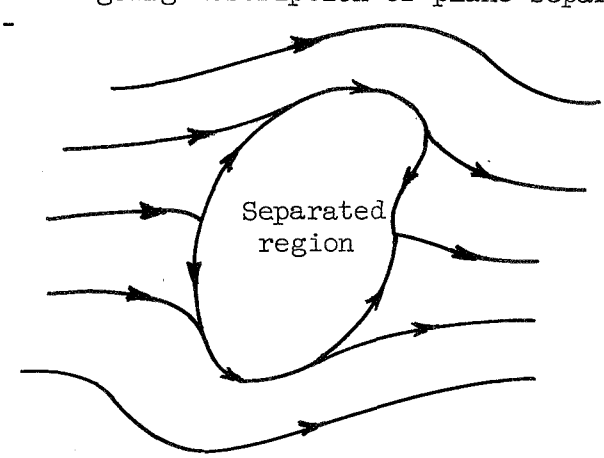

(g) Separation in three-dimensional flow with reattachment.

and reattachment in plane flow. If somewhere within or at the boundary of the separated region the theoretical boundary-layer solution would a priori be expected to blow up, then the vortex system within the separated region is free to roll up into a more or less vigorous system of vortices.

Thus, thin-boundary-layer theory can be used to obtain the following information concerning laminar separation:

(1) The solution may establish the existence of a vortex sheet which is embedded in a flat bubble on the surface and which could adhere to the surface and remain part of a thin boundary layer, provided that the Prandtl equations are valid everywhere in the separated region.

(2) The solution might predict the boundary layer to go to infinite thickness somewhere in the separated region. If this happens, then the separated region is free to roll up, thus providing a vigorous wake (which, of course, is not amenable to boundary-layer theory).

For flow about a plane body, the boundary-layer solution is not needed for predicting the breakdown of the Prandtl assumptions. Physical considerations suffice to establish where (at stagnation point of outer flow) and when (always) the breakdown occurs. In three-dimensional flow this is not always so clear, and at least certain features of the solution are required to be known. In order that the boundary-layer equations be applicable, the solution must be such that the boundary layer entrains fluid (that is, flow streamlines enter, but do not leave, the boundary layer at its outer edge). In a cartesian system, where $h(x,z)$ is the outer edge of the boundary layer, this requirement may be written as

$$u_1 h_x + w_1 h_z > (v_1)_{y=h} \tag{32}$$

Equations (32) and (28) may be combined with the equation of continuity in the form

$$\rho_1 \left(\frac{\partial v_1}{\partial y}\right)_{y=0} = -\left[(\rho_1 u_1)_x + (\rho_1 w_1)_z\right]$$

to yield

$$\frac{\partial}{\partial x}\left[(h - \Delta)\rho_1 u_1\right] + \frac{\partial}{\partial z}\left[(h - \Delta)\rho_1 w_1\right] > 0$$

or, in vector notation,

$$\operatorname{div}\left[(h - \Delta)\rho_1 \underline{q}_1\right] > 0 \tag{33}$$

where Δ is the displacement thickness, and $\underline{q}_1$ is the velocity vector in the outer flow evaluated at the body surface.

In many cases, circumstances may be found for which inequality (33) cannot be satisfied. For example, for plane incompressible flow about a cylinder and, as is customary, with u and x defined parallel to the surface, inequality (33) may be written

$$\frac{\frac{d}{dx}(h - \Delta)}{h - \Delta} > \frac{-\frac{du_1}{dx}}{u_1}$$

As the rear stagnation point of the outer flow is approached, u_1 tends to zero, while $-du_1/dx$ remains finite and positive. Therefore, since $h - \Delta$ by definition must be greater than zero, $d(h - \Delta)/dx$ must approach infinity in clear violation of the boundary-layer assumptions.

Separation on Cone at Angle of Attack

In the previous discussion, it was concluded that separation involving a strong vortex pattern occurs if a tentative boundary-layer solution predicts an embedded vortex sheet coupled with a local breakdown of the assumption of a thin boundary layer. In the case of the cone, inequality (33) may be used to predict the circumstances under which the boundary layer may not be regarded as thin: When the fact of parabolic similarity is introduced ($h - \Delta$ proportional to $\sqrt{x}$), inequality (33) becomes

$$\frac{\frac{\partial}{\partial \varphi}(h - \Delta)}{h - \Delta} > \frac{-w_{1_\varphi} - \frac{3}{2}\theta u_1}{w_1} \tag{34}$$

This inequality indicates infinite boundary-layer thickness only when $w_1 = 0$ and, even then, only if w_{1_φ} is negative (which is true at the top of the cone, $\varphi = \pi$) and larger in magnitude than $\frac{3}{2}\theta u_1$. This is true only for angles of attack larger than that for which $k = -1$ (by equation (10b)). When the angle of attack is smaller than this critical value, the right member of inequality (34) is always negative, and $\partial(h - \Delta)/\partial\varphi$ may be considered to vanish by symmetry at $\varphi = \pi$ without violating inequality (34).

The foregoing result may be explained on physical grounds as follows: As the boundary layer proceeds around the cone, it entrains fluid which it then conveys towards the top (symmetrically, from both sides of the cone). In the plane cylinder case, the fluid similarly conveyed must finally erupt

from the boundary layer when the stagnation point is reached. However, on the cone, the boundary layer grows parabolically along generators; and, hence, if the cross-flow is not too strong (small angle of attack), the fluid brought to the top may simply become part of the growing boundary layer. For larger angles of attack, the boundary layer cannot grow at a rate sufficient to absorb the additional fluid, and eruption occurs with the consequent breakdown of the thin-boundary-layer assumptions.

Accordingly, it is proposed that when the angle of attack is less than that for which $k = -1$, a thin boundary layer covers the cone (fig. 3(a)). For larger angles of attack, any vortex sheet present will roll up to form attached lobes (fig. 3(b)); for still larger angles of attack, a vortex street is produced.

Thus when $k < -1$ (angle of attack greater than that for which $k = 1$), strong viscous cross forces (viscous lift) on the cone may be expected. These forces are discussed by Allen in reference 13. Of course, a weakness of the present analysis is that no indication is given as to the strength of the rolled-up vortex system because, when $k = -1$, the presence of an embedded vortex sheet over the top part of the cone has not been established. It seems likely that such a vortex sheet does exist because a rather strong adverse pressure gradient (fig. 2(b)) always exists when $k = -1$. In fact, it may be shown (most conveniently by evaluating equation (7a) at $\lambda = \infty$) that an adverse pressure gradient exists when $k < -2/3$.

Equations (35), (13), (14), and (10b) give the minimum angle of attack for which the boundary layer may be expected to break away from the surface and to form lobes at the top of the cone. This angle is presented as a function of stream Mach number and vertex angle. Figure 9 shows the results of such a calculation. The critical angle of attack is given as a ratio of angle of attack to semivertex angle for convenience. The results show that, in general, separation involving lobes occurs later (in terms of relative angle of attack α/θ) for the smaller vertex angles, particularly at higher Mach numbers. Figure 9 indicates the possibility of rather profound qualitative differences in the flows at high Mach number about cones of different vertex angles.

The foregoing interpretation of the critical condition $k = -1$ is supported by the experimental result shown in figure 4. From figure 5, $k = -1$ when $\alpha = 6.2^\circ$, under the conditions of the test. Figure 4(b) shows the measured total head rising as the angle of attack is increased beyond 6.2°. Presumably this effect is caused by the the induced field of the symmetrical pair of vortex lobes sweeping away the thick boundary layer between, thus reestablishing a thin boundary layer at the top of the cone.

It may be of interest to note that if similarity also holds for the turbulent boundary layer on a cone, and the similarity law is nearly linear (rather than parabolic as in the laminar case), separation would first appear at a higher angle of attack than in laminar flow. In fact, equations (10b) and (31) or (33) would yield the criterion $k = -4/3$.

For the boundary layer produced by supersonic flow over any smooth conically symmetric body in supersonic flow (such as a cone of elliptic cross section), inequality (33) and the condition of parabolic boundary-layer similarity may be used to find a criterion equivalent to $k = -1$ for the maximum angle of attack consistent with a thin boundary layer.

CONCLUSIONS

The laminar boundary-layer flow about a circular cone at large angles of attack to a supersonic stream has been analyzed in the plane of symmetry with the following results:

1. At the bottom of the cone, profiles of meridional velocity and of the gradient of circumferential velocity were determined and showed the expected tendency of the boundary layer to become thinner on the underside of the cone as the angle of attack is increased.

2. At the top of the cone, except for very small angles of attack, the analysis (which is restricted to the plane of symmetry) failed for the following reasons:

(a) For angles of attack greater than some rather small value, the boundary layer brings information from beneath the cone into the vicinity of the plane of symmetry at the top. Therefore, the analysis, which deals only with the plane of symmetry, yielded indeterminate solutions.

(b) For angles of attack greater than some angle (roughly of the order of the cone semivertex angle), no boundary-layer solution is possible. The characteristics of the outer flow and the known parabolic similarity of the boundary layer would together imply that, beyond this critical angle, there would be a component of flow leaving the boundary layer. This is physically impossible, since a boundary layer always entrains fluid. Thus, beyond the critical angle of attack, no solution can exist for equations which presume a thin boundary layer.

For three-dimensional flow it is proposed that a separated region be regarded as a vortex sheet embedded in the boundary layer, remaining flat against the body if the assumption of a thin boundary layer is valid throughout the region. If, however, the boundary-layer assumptions break down anywhere in the separated region, it is inferred that the vortex sheet may roll up to form strong vortices which may either remain attached or be shed as a vortex street.

On the cone, therefore, the critical angle of attack beyond which no boundary-layer solution is possible at the top of the cone represents the maximum angle of attack for which the boundary layer is everywhere thin or, alternatively, the minimum angle of attack for which major disruption of the flow may be expected because of the formation of strong vortex lobes. Beyond this angle of attack, strong viscous cross forces may be anticipated.

A similar criterion could easily be obtained for the boundary layer on any smooth conically symmetric body in supersonic flow.

The assumption of a suitable similarity law suffices to establish a similar criterion if the boundary layer on a conical body is turbulent.

Lewis Flight Propulsion Laboratory
National Advisory Committee for Aeronautics
Cleveland, Ohio, September 15, 1952

APPENDIX A

SYMBOLS

The following symbols are used in this report:

C	constant appearing in temperature-viscosity relation (equation (5a))
C_{f_x}	component of skin-friction coefficient in x-direction
C_{f_φ}	component of skin-friction coefficient in φ-direction
c_p	specific heat at constant pressure
$F(\lambda)$	function appearing in asymptotic representation of f (equations (24))
$f(\lambda,\varphi)$	function related to meridional velocity u by equation (2)
$g(\lambda,\varphi)$	function related to circumferential velocity w by equation (2)
h	height of outer edge of boundary layer
k	related to circumferential gradient of circumferential velocity in plane of symmetry (equation (10b))
M	Mach number
p	static pressure
$\underline{q}_1$	velocity vector at outer edge of boundary layer
R_x	Reynolds number, $\rho_1 u_1 x/\mu_1$
$R_\Delta, R_{\delta_x}, R_{\delta_\varphi}$	Reynolds numbers, $\rho_1 u_1 \Delta/\mu_1$, $\rho_1 u_1 \delta_x/\mu_1$, $\rho_1 u_1 \delta_\varphi/\mu_1$, respectively
T	absolute static temperature
u	meridional component of velocity
v	component of velocity normal to surface
w	circumferential velocity component

x	coordinate along generators of cone
y	coordinate normal to surface
α	angle of attack (positive as shown in fig. 1)
γ	ratio of specific heats
Δ	displacement surface
δ_x	mass-flow defect associated with meridional velocity profile (equation (21))
δ_φ	mass-flow defect associated with circumferential profile (equation (21))
Θ	semivertex angle of cone
θ	sine of semivertex angle of cone
λ	dimensionless variable (equation (3))
μ	coefficient of viscosity
ρ	density
φ	angular coordinate around cone
$\Psi(\lambda)$	function appearing in asymptotic representation of ψ (equations (24))
$\psi(\lambda)$	function related to circumferential velocity w in plane of symmetry by equation (10a)

Subscripts:

max	maximum
r	reference condition, nonviscous flow at surface, at $\varphi = 0$ or $\varphi = \pi$, whichever is appropriate
1	evaluation at outer edge of boundary layer (alternatively, nonviscous flow at surface)

Subscript notation for partial differentiation has been used

Superscripts:

$'$	Primes denote ordinary differentiation with respect to λ or φ
$-$	Bar over quantity indicates evaluation of nonviscous flow at surface when cone is at zero angle of attack

APPENDIX P

NUMERICAL SOLUTION OF DIFFERENTIAL EQUATIONS

By Lynn Albers

The two simultaneous nonlinear ordinary differential equations (11a) and (11b) together with boundary conditions (12) constitute a two-point boundary value problem. The method of numerical solution used applies directly only to problems fow which all boundary conditions are specified at a single initial point (the origin, in the present case). Each numerical integration was therefore performed starting with boundary conditions (12a) and (12b) and a tentative specification of $f''(0)$ and $\psi''(0)$. In each case, such integration was carried out for a sufficient variety of conditions $f''(0)$ and $\psi''(0)$ so that the correct set of initial conditions yielding the proper behavior at $\lambda = \infty$ (boundary condition (12a)) could be inferred to the desired degree of accuracy.

Integration was performed according to the following basic scheme: With the values of $f'''(\lambda)$ and $\psi'''(\lambda)$ given at five closely spaced values of λ, fourth-degree polynomials may be passed through the two sets of values of f''' and ψ'''. Then, if f, f', f'', ψ, ψ', and ψ'' are known at the fifth point, the polynomial representations of f''' and ψ''' may be integrated to yield f, f', f'', ψ, ψ', and ψ'' at the next (sixth) point. These quantities may then be substituted into differential equations (11) to yield f''' and ψ''' at the sixth point. In this way, the solution may be extended one step at a time, in each step by use of the solution at the five previous points. In order to begin this procedure, the solution must first be found at five points starting at the origin and must be subject to boundary conditions (12b) and (12c) and the tentative selection of $f''(0)$ and $\psi''(0)$.

This preliminary calculation was done in the following manner: $f'''(0)$ was calculated directly from equations (11) and (12) and was used as an initial estimate of f''' at the next four points. Given $f(0)$, $f'(0)$, and $f''(0)$, the values of f, f', and f'' were computed at the second point by integrating a fourth-degree polynomial passed through the five values of f'''. In a similar manner, ψ, ψ', and ψ'' at the second point were found. Direct substitution into equations (11) then yields improved estimates for f''' and ψ''' at the second point and thus an improved polynomial representation of these functions which may be used to obtain values of f, f', f'', ψ, ψ', and ψ'' at the second point, and so forth, until improved values have been obtained at the fifth point. This procedure was repeated in an iterative manner until convergence was obtained at each of the five initial points.

All calculations were performed on the IBM Card Programmed Electronic Calculator. Results are considered correct to four significant figures.

REFERENCES

1. Anon.: Tables of Supersonic Flow Around Cones. Tech. Rep. No. 1, Dept. Elec. Eng., M.I.T., 1947.

2. Anon.: Tables of Supersonic Flow Around Yawing Cones. Tech. Rep. No. 3, Dept. Elec. Eng., M.I.T., 1947.

3. Anon.: Tables of Supersonic Flow Around Cones of Large Yaw. Tech. Rep. No. 5, Dept. Elec. Eng., M.I.T., 1949.

4. Young, G. B. W., and Siska, C. P.: Supersonic Flow Around Cones at Large Yaw. Jour. Aero. Sci., vol. 19, no. 2, Feb. 19, 1952, pp. 111-119.

5. Hayes, Wallace D.: The Three-Dimensional Boundary Layer. NAVORD Rep. 1313, NOTS 384, U.S. Naval Ordnance Test Station (Inyokern), May 9, 1951. (Bur. Ordnance Task Assignment NOTS-36-Re3d-441-3.)

6. Moore, Franklin K.: Three-Dimensional Compressible Laminar Boundary-Layer Flow. NACA TN 2279, 1951.

7. Moore, Franklin K.: Laminar Boundary Layer on a Circular Cone in Supersonic Flow at a Small Angle of Attack. NACA TN 2521, 1951.

8. Moore, Franklin K.: Use of the Boundary Layer of a Cone to Measure Supersonic Flow Inclination. NACA TN 2723, 1952.

9. Chapman, Dean R., and Rubesin, Morris W.: Temperature and Velocity Profiles in the Compressible Laminar Boundary Layer with Arbitrary Distribution of Surface Temperature. Jour. Aero. Sci., vol. 16, no. 9, Sept. 1949, pp. 547-565.

10. Ferri, Antonio: Supersonic Flow Around Circular Cones at Angles of Attack. NACA TN 2236, 1950.

11. Moore, Franklin K.: Displacement Effect of a Three-Dimensional Boundary Layer. NACA TN 2722, 1952.

12. Whittaker, E. T., and Watson, G. N.: Modern Analysis. The Macmillan Co. (New York), 1943.

13. Allen, H. Julian: Pressure Distribution and Some Effects of Viscosity on Slender Inclined Bodies of Revolution. NACA TN 2044, 1950.

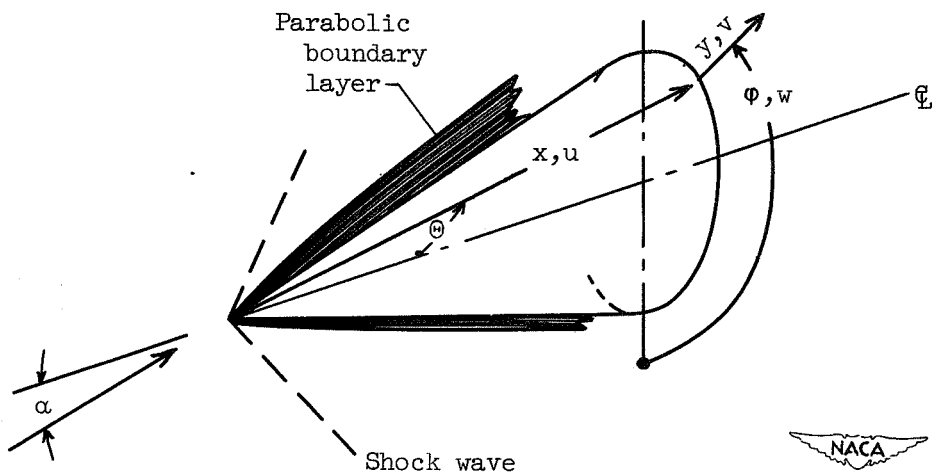

Figure 1. - Cone at angle of attack to supersonic stream.

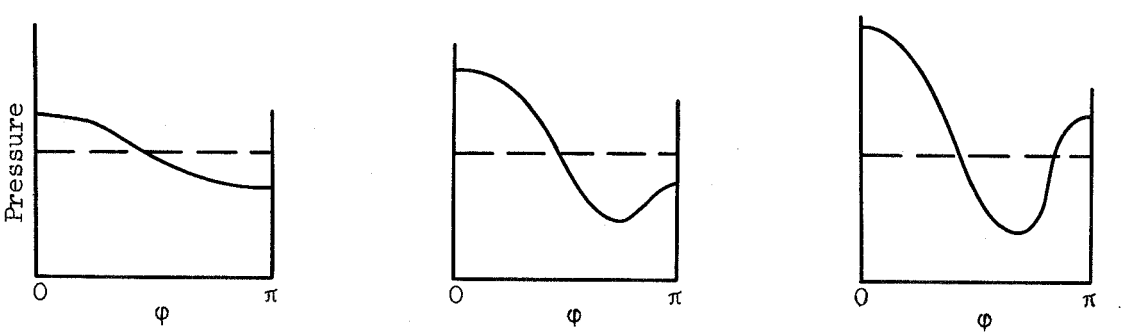

(a) Small α. (b) Moderate α. (c) Large α.

Figure 2. - Pressure distribution around cone for various ranges of angle of attack.

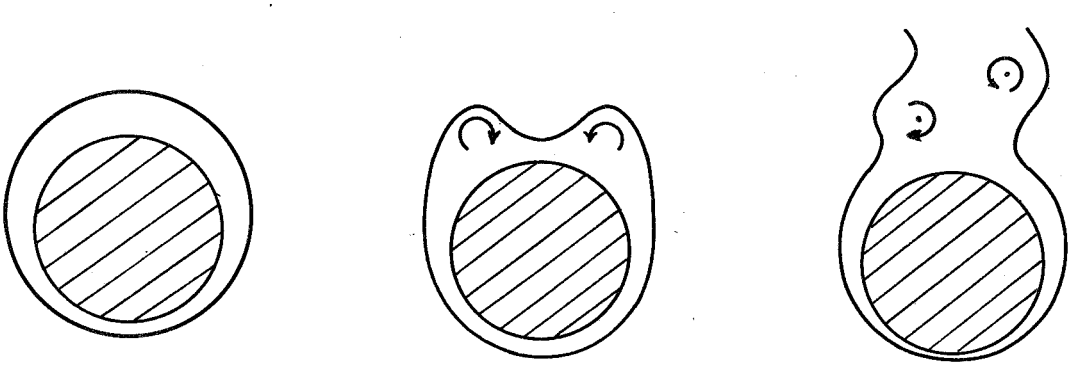

(a) Small α. (b) Moderate α. (c) Large α.

Figure 3. - Cross-sectional views of boundary layer on cone at various angles of attack.

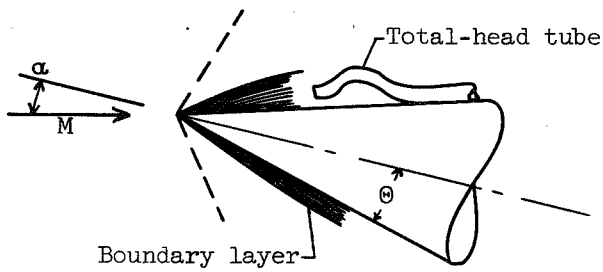

(a) Test configuration.

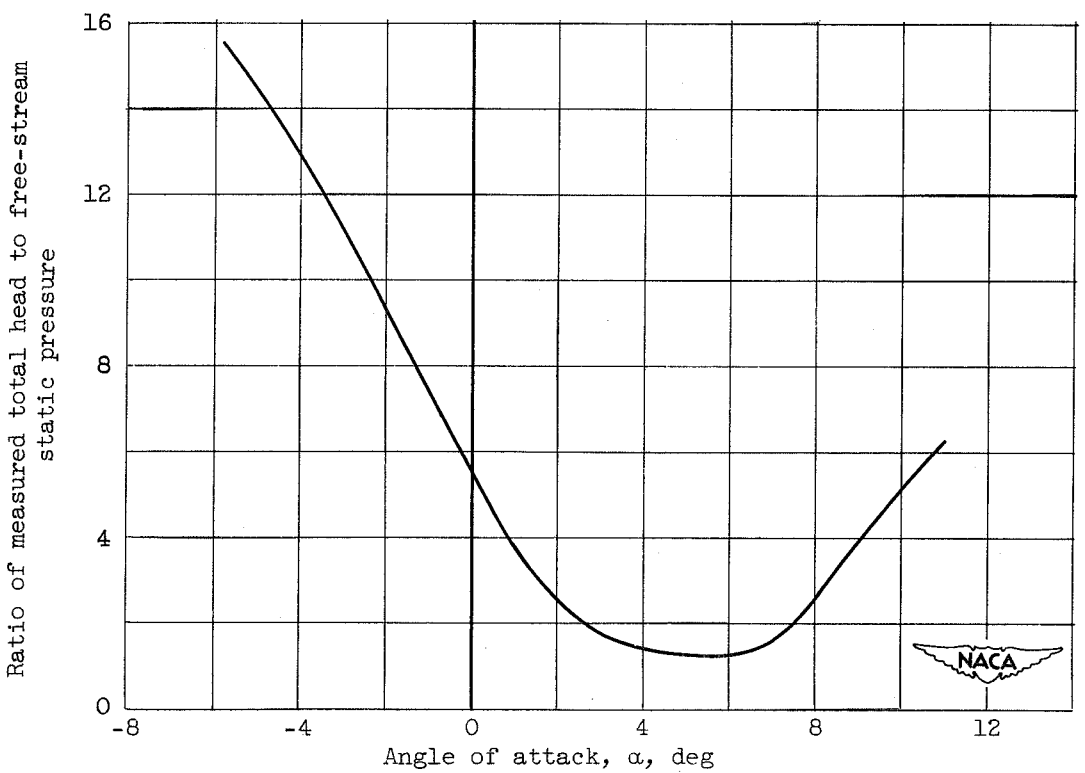

(b) Variation of total head with angle of attack.

Figure 4. - Variation with angle of attack of total head measured in boundary layer of cone. M, 3.095; Θ, 7.5°.

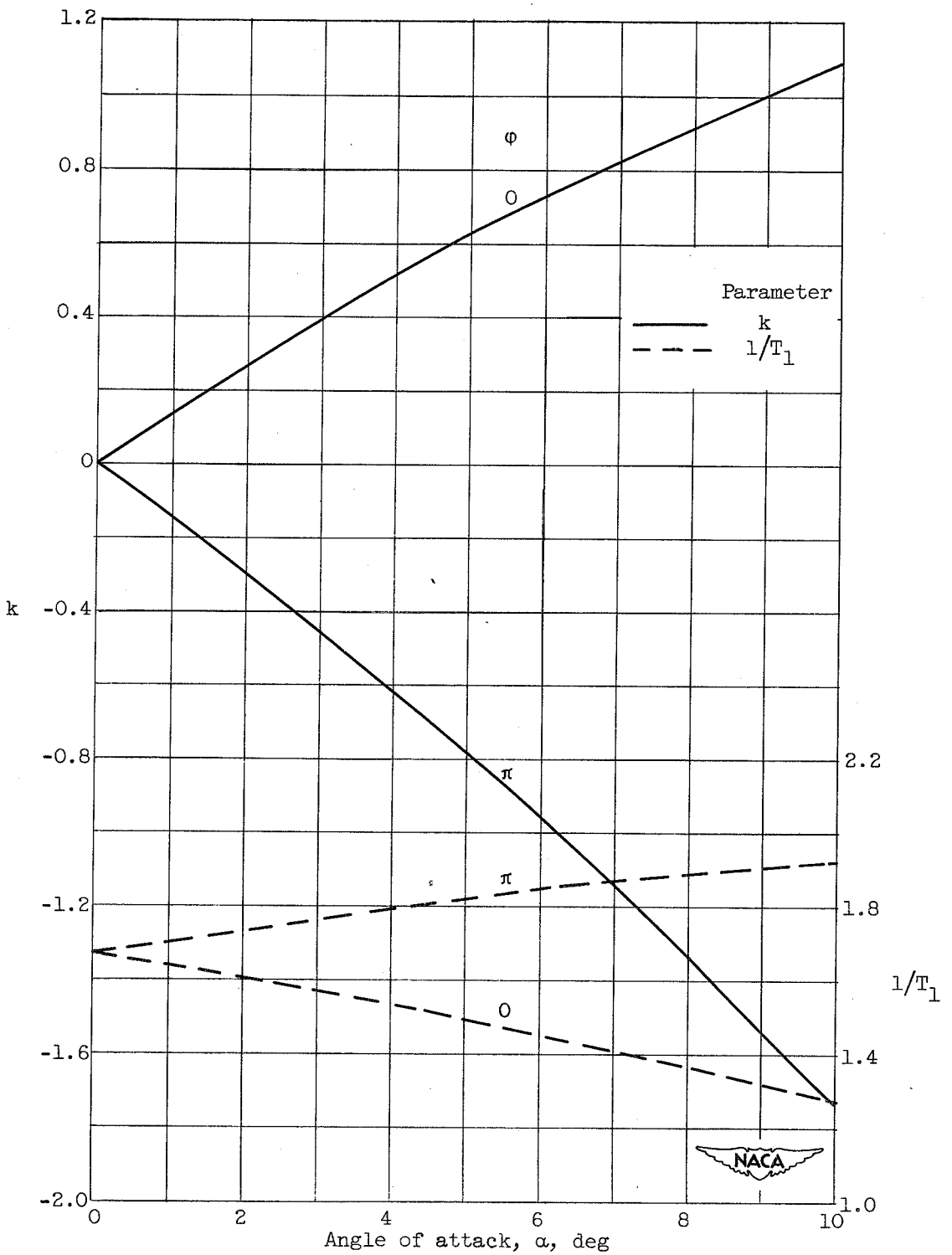

Figure 5. - Variation of parameters k and $1/T_1$ with angle of attack. M, 3.1; Θ, 7.5°.

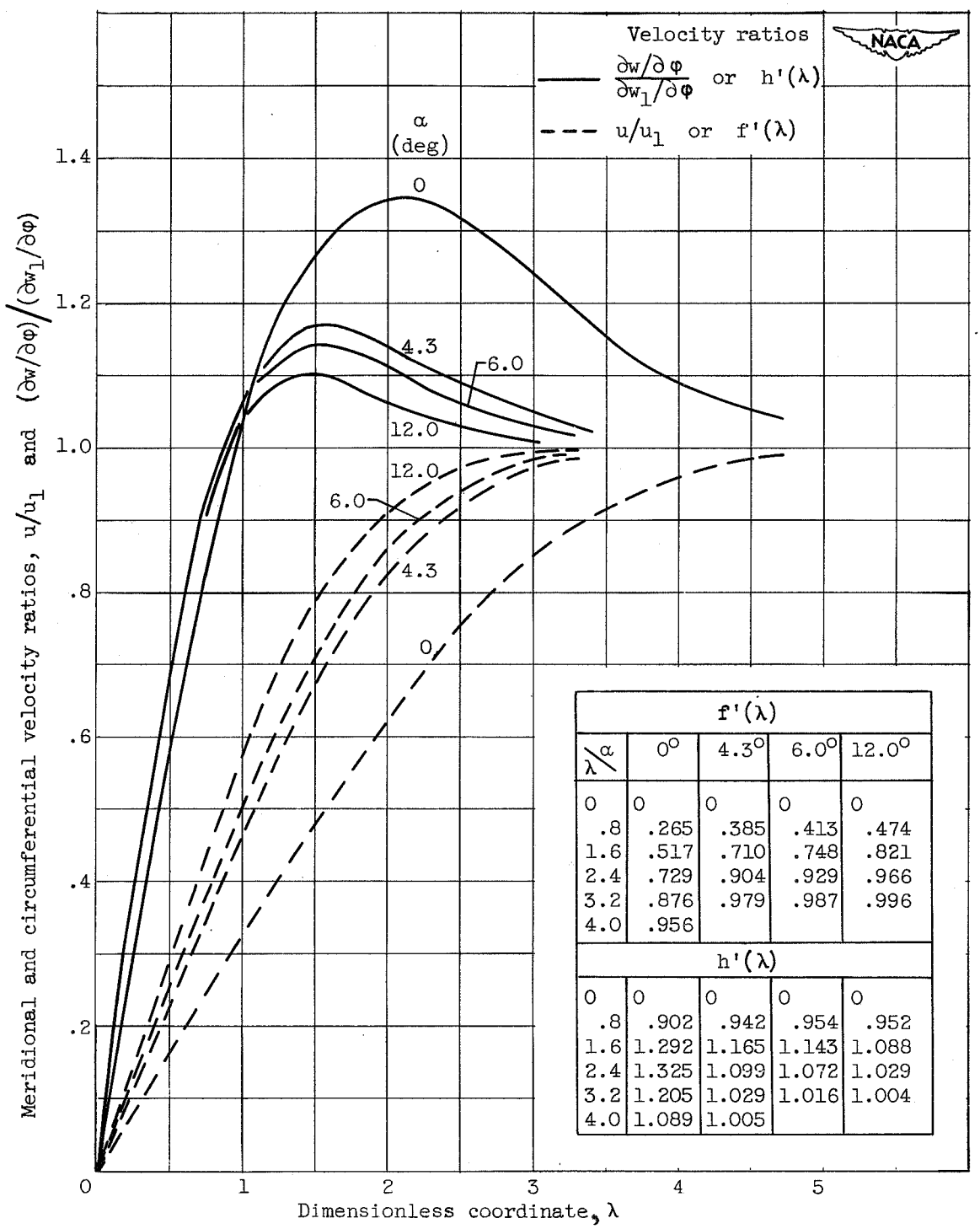

f'(λ)				
λ / α	0°	4.3°	6.0°	12.0°
0	0	0	0	0
.8	.265	.385	.413	.474
1.6	.517	.710	.748	.821
2.4	.729	.904	.929	.966
3.2	.876	.979	.987	.996
4.0	.956			

h'(λ)				
0	0	0	0	0
.8	.902	.942	.954	.952
1.6	1.292	1.165	1.143	1.088
2.4	1.325	1.099	1.072	1.029
3.2	1.205	1.029	1.016	1.004
4.0	1.089	1.005		

Figure 6. - Velocity profiles at $\varphi = 0$. M, 3.1; Θ, 7.5°.

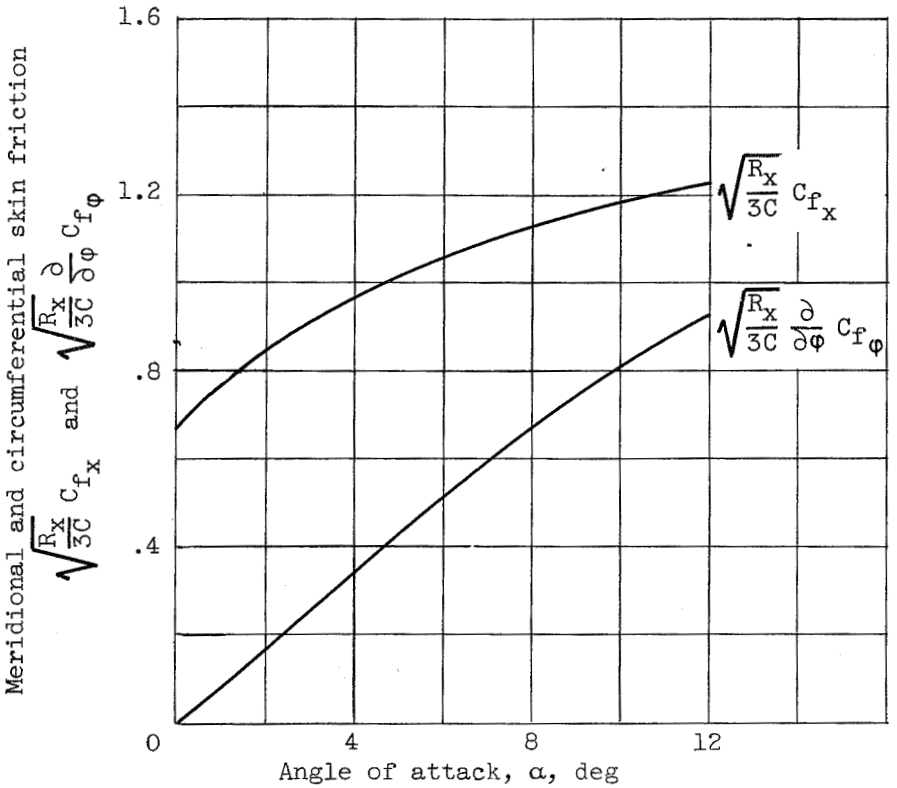

Figure 7. - Meridional and circumferential skin-friction coefficients at $\varphi = 0$. M, 3.1; Θ, 7.5°.

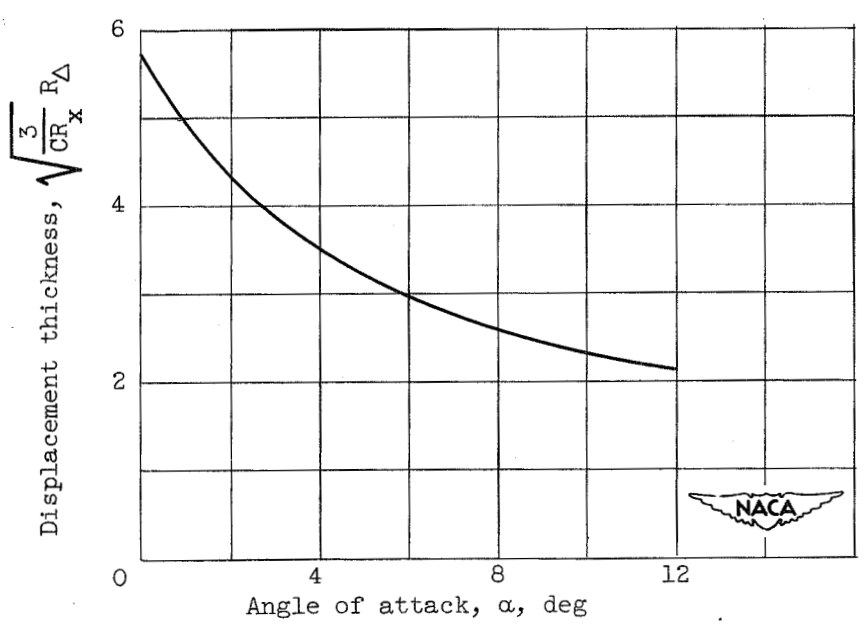

Figure 8. - Displacement thickness at $\varphi = 0$. M, 3.1; Θ, 7.5°.

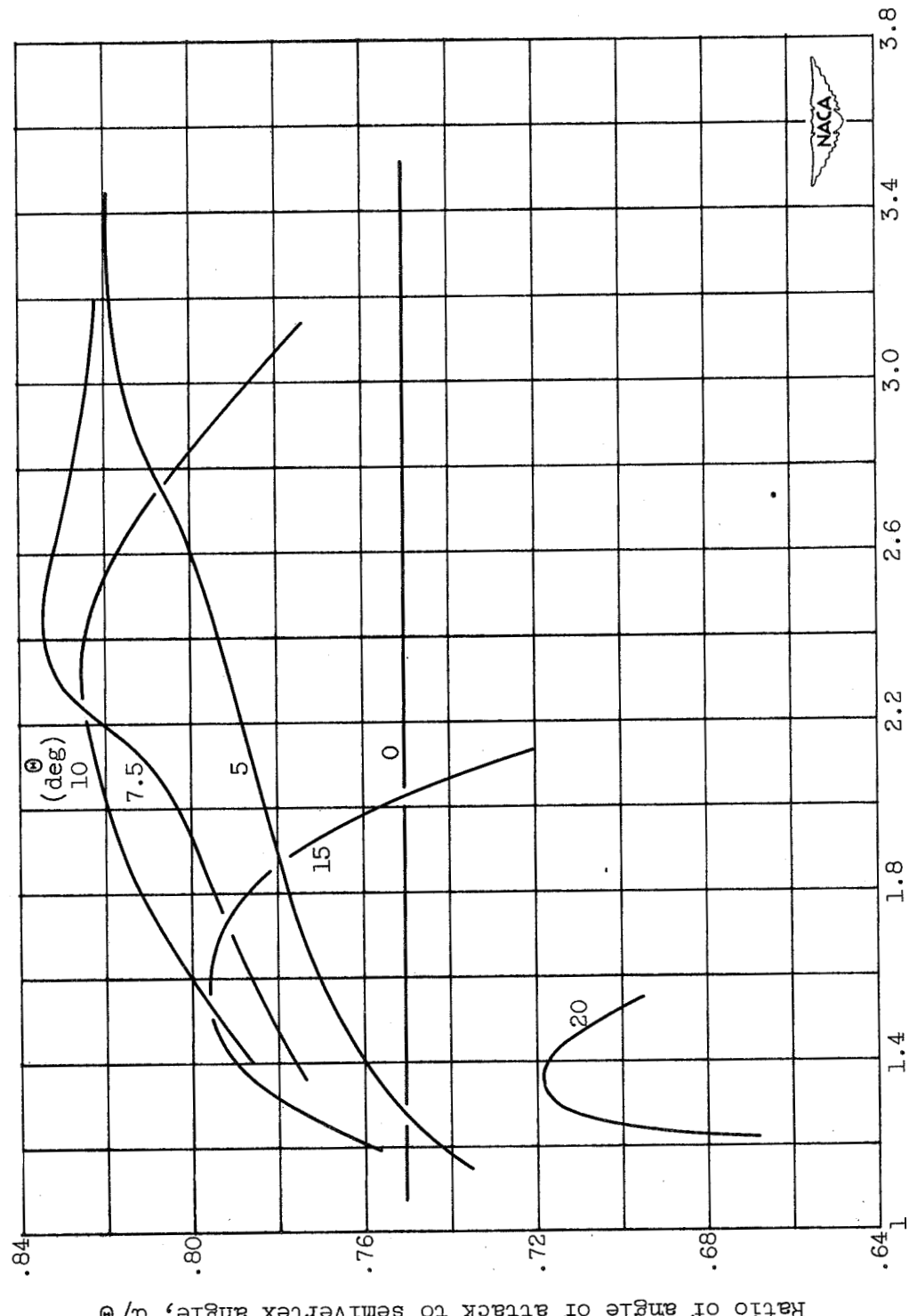

Figure 9. - Minimum angle of attack for which separation appears at $\varphi = \pi$.